9

Force Control

Solution to Problem 9.1

Computing the time derivative of $\boldsymbol{o}_{d,e}^{d} = \boldsymbol{R}_{d}^{T}(\boldsymbol{o}_{e} - \boldsymbol{o}_{d})$ gives

$$\dot{\boldsymbol{o}}_{d,e}^{d} = \boldsymbol{R}_{d}^{T}(\dot{\boldsymbol{o}}_{e} - \dot{\boldsymbol{o}}_{d}) - \dot{\boldsymbol{R}}_{d}^{T}(\boldsymbol{o}_{e} - \boldsymbol{o}_{d}). \tag{S9.1}$$

In view of (3.10), (3.7) and (3.11) the following equality holds

$$\dot{\boldsymbol{R}}_{d}^{T} = -\boldsymbol{R}_{d}^{T}\boldsymbol{S}(\boldsymbol{\omega}_{d}) = -\boldsymbol{S}(\boldsymbol{R}_{d}^{T}\boldsymbol{\omega}_{d})\boldsymbol{R}_{d}^{T} = -\boldsymbol{S}(\boldsymbol{\omega}_{d}^{d})\boldsymbol{R}_{d}^{T} \tag{S9.2}$$

which, replaced in (S9.1), gives (9.10).

To derive (9.11), consider the equality

$$\dot{\boldsymbol{R}}_{e}^{d} = \dot{\boldsymbol{R}}_{d}^{T}\boldsymbol{R}_{e} + \boldsymbol{R}_{d}^{T}\dot{\boldsymbol{R}}_{e} = -\boldsymbol{S}(\boldsymbol{\omega}_{d}^{d})\boldsymbol{R}_{d}^{e} + \boldsymbol{S}(\boldsymbol{\omega}_{e}^{d})\boldsymbol{R}_{d}^{e} = \boldsymbol{S}(\boldsymbol{\omega}_{d,e}^{d})\boldsymbol{R}_{d}^{e},$$

where (S9.2), (3.10), and (3.11) have been used. It follows that (3.64) can be rewritten as

$$\boldsymbol{\omega}_{d,e}^{d} = \boldsymbol{T}(\boldsymbol{\phi}_{d,e})\dot{\boldsymbol{\phi}}_{d,e}$$

being $\boldsymbol{\phi}_{d,e}$ the vector of Euler angles extracted from $\boldsymbol{R}_{e}^{d}$ and $\boldsymbol{\omega}_{d,e}^{d}$ the angular velocity corresponding to $\dot{\boldsymbol{R}}_{e}^{d}$. Hence, expression (9.11) follows.

Solution to Problem 9.2

Pre-multiplying by $\boldsymbol{K}$ both sides of the equality

$$d\boldsymbol{x}_{r,e} = d\boldsymbol{x}_{r,d} - d\boldsymbol{x}_{e,d},$$

and using (9.21) and (9.20) gives

$$\boldsymbol{h}_{e} = \boldsymbol{K}d\boldsymbol{x}_{r,d} - \boldsymbol{K}\boldsymbol{K}_{P}^{-1}\boldsymbol{h}_{e}$$

and thus

$$(\boldsymbol{I}_6 + \boldsymbol{K}\boldsymbol{K}_P^{-1})\boldsymbol{h}_e = \boldsymbol{K}d\boldsymbol{x}_{r,d},$$

from which expression (9.22) follows. Equality (9.23) is obtained replacing (9.22) into (9.20).

Solution to Problem 9.3

Similarly to Example 9.2, all the quantities can be referred to a base frame and control law with force measurement (9.30), (9.31) can be adopted. To compute the model of the contact force, in view of the geometry of the environment, it is useful to consider also a rotated base frame with axes parallel to the axes x_c and y_c of Fig. 9.16 and with the same origin of the base frame of axes x_0 and y_0. The corresponding rotation matrix is

$$\boldsymbol{R}_c = \begin{bmatrix} 1/\sqrt{2} & -1/\sqrt{2} \\ 1/\sqrt{2} & 1/\sqrt{2} \end{bmatrix}.$$

In the rotated base frame, the environment stiffness matrix has the simple expression

$$\boldsymbol{K}^c = \mathrm{diag}\{0, k_y\},$$

corresponding to the absence of interaction forces along the direction of axis x_c ($\boldsymbol{f}_e^c = [\,0 \quad f_y^c\,]^T$). The elastic force in the rotated base frame has the expression

$$\boldsymbol{f}_e^c = \boldsymbol{K}^c(\boldsymbol{o}_e^c - \boldsymbol{o}_r^c),$$

being $\boldsymbol{o}_e^c$ the end-effector position and $\boldsymbol{o}_r^c$ the equilibrium position of the plane in the rotated base frame. The above expression can be rewritten in the base frame in the form

$$\boldsymbol{f}_e = \boldsymbol{K}(\boldsymbol{o}_e - \boldsymbol{o}_r),$$

with

$$\boldsymbol{K} = \boldsymbol{R}_c\boldsymbol{K}^c\boldsymbol{R}_c^T = k_y \begin{bmatrix} 1/2 & -1/2 \\ -1/2 & 1/2 \end{bmatrix}$$

and $\boldsymbol{o}_r = [\,1 \quad 0\,]^T$.

The impedace parameters can be set similarly to Example 9.2, on the basis of the equations

$$\begin{aligned} m_{dx}\ddot{x}_e^c + k_{Dx}\dot{x}_e^c + k_{Px}x_e^c &= k_{Px}x_d^c \\ m_{dy}\ddot{y}_e^c + k_{Dy}\dot{y}_e^c + (k_{Py} + k_y)y_e^c &= k_y y_r^c + k_{Py}y_d^c \end{aligned}$$

referred to the rotated base frame, where the diagonal matrices

$$\boldsymbol{M}_d^c = \mathrm{diag}\{m_{dx}, m_{dy}\} \qquad \boldsymbol{K}_D^c = \mathrm{diag}\{k_{Dx}, k_{Dy}\} \qquad \boldsymbol{K}_P^c = \mathrm{diag}\{k_{Px}, k_{Py}\}$$

define an active impedance in the rotated base frame. The corresponding impedance matrices referred to the base frame are

$$\boldsymbol{M}_d = \boldsymbol{R}_c\boldsymbol{M}_d^c\boldsymbol{R}_c^T \qquad \boldsymbol{K}_D = \boldsymbol{R}_c\boldsymbol{M}_d^c\boldsymbol{R}_c^T \qquad \boldsymbol{K}_P = \boldsymbol{R}_c\boldsymbol{M}_d^c\boldsymbol{R}_c^T.$$

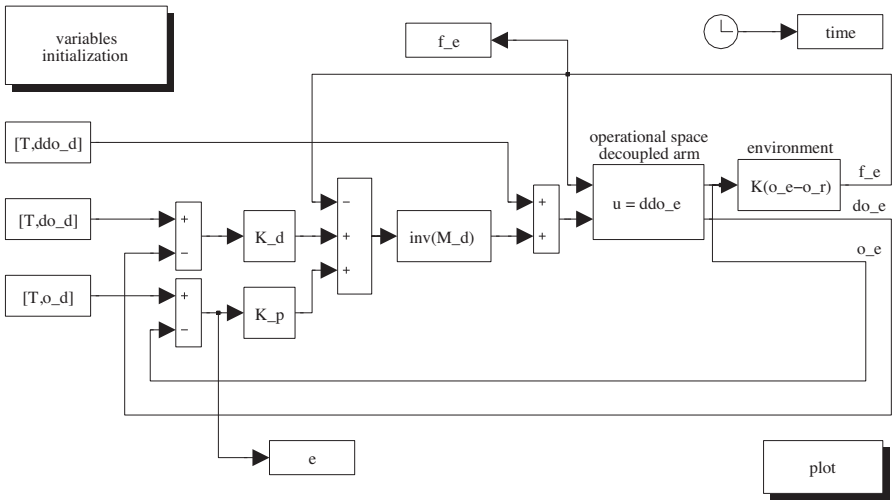

Fig. S9.1. SIMULINK block diagram of impedance control.

Notice that, differently from Example 9.2, the interaction occurs along y_c. Therefore, for the unconstrained motion along x_c, the behaviour is determined by

$$\omega_{nx} = \sqrt{\frac{k_{Px}}{m_{dx}}} \qquad \zeta_x = \frac{k_{Dx}}{2\sqrt{m_{dx}k_{Px}}},$$

while, for the constrained motion along axis y_c, the behaviour is determined by

$$\omega_{ny} = \sqrt{\frac{k_{Py} + k_y}{m_{dy}}} \qquad \zeta_y = \frac{k_{Dy}}{2\sqrt{m_{dy}(k_{Py} + k_y)}}.$$

With the choice

$$m_{dx} = m_{dy} = 100 \qquad k_{Dx} = k_{Dy} = 1600 \qquad k_{Px} = k_{Py} = 5000,$$

and the given value of environment stiffness k_y, the dynamics is characterized by

$$\omega_{nx} = 7.07\,\text{rad/s} \qquad \zeta_x = 1.13$$

and

$$\omega_{ny} = 10\,\text{rad/s} \qquad \zeta_y = 0.8.$$

The desired tip trajectory is generated in terms of the path coordinate s via a trapezoidal velocity profile with maximum velocity $\dot{s}_c = 0.5$.

The resulting SIMULINK block diagram is shown in Fig. S9.1. The arm is simulated as a continuous-time system using the a variable-step integration method with a minimum step size of 1 ms. All the blocks of the controller are simulated as discrete-time subsystems with the given sampling time of 1 ms.

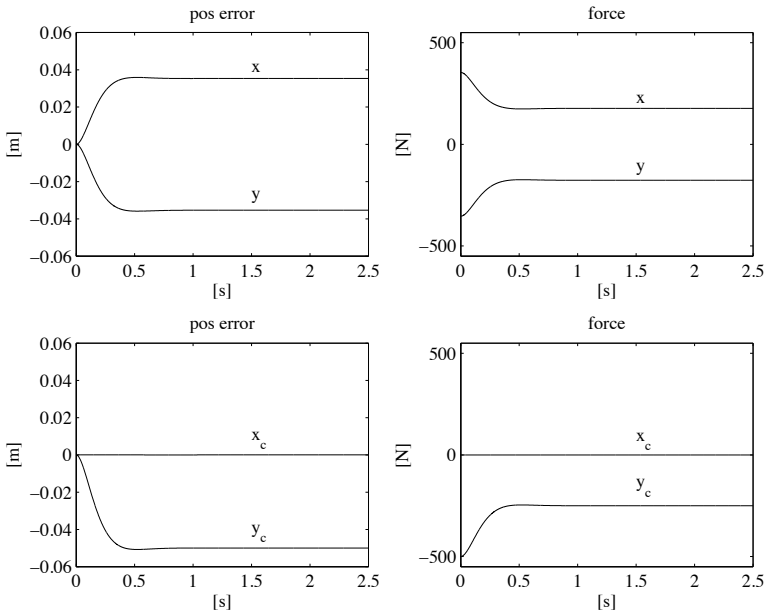

Fig. S9.2. Time history of the tip position error and of the contact force with impedance control. Top: components in the base frame. Bottom: components in the rotated base frame.

The files with the solution can be found in Folder `9_3`.

The resulting tip position error and contact force are shown in Fig. S9.2, both referred to the base frame (top) and to the rotated base frame (bottom). It can be verified that the position error keeps small during the task execution, ensuring a bounded contact force. In particular, it can be observed that the position error is null along the unconstrained motion direction (axis x_c), where the force is null; on the other hand, the force response along the constrained motion direction (axis y_c) remains bounded and converges to a constant value which depends on the plane stiffness and undeformed position as well as on the active compliance.

Solution to Problem 9.4

From the block scheme in Fig. 9.8, at the equilibrium, it is $\dot{\boldsymbol{x}} \equiv \boldsymbol{0}$, $\ddot{\boldsymbol{x}} \equiv \boldsymbol{0}$. Then, the input to the block $\boldsymbol{K}_P$ must be null, which implies

$$\boldsymbol{x}_d + \boldsymbol{x}_F - \boldsymbol{x}_e = \boldsymbol{0}.$$

In view of (9.21) and (9.41), it follows that

$$\boldsymbol{x}_d + \boldsymbol{C}_F\big(\boldsymbol{K}(\boldsymbol{x}_r - \boldsymbol{x}_e) + \boldsymbol{f}_d\big) - \boldsymbol{x}_e = \boldsymbol{0},$$

and thus the equilibrium location satisfies the equation

$$\boldsymbol{x}_e = \boldsymbol{x}_d + \boldsymbol{C}_F\big(\boldsymbol{K}(\boldsymbol{x}_r - \boldsymbol{x}_e) + \boldsymbol{f}_d\big).$$

Solution to Problem 9.5

The norm of vector

$$\boldsymbol{\epsilon} = \boldsymbol{h}_e - \boldsymbol{S}_f\boldsymbol{\lambda}$$

with weighting matrix $\boldsymbol{W}$ is defined as

$$\|\boldsymbol{\epsilon}\|_W = \sqrt{\boldsymbol{\epsilon}^T\boldsymbol{W}\boldsymbol{\epsilon}}. \tag{S9.3}$$

The vector $\boldsymbol{\lambda}$ which minimizes the norm (S9.3) can computed also as the solution of a minimization problem for the quadratic cost functional

$$g(\boldsymbol{\epsilon}) = \frac{1}{2}\boldsymbol{\epsilon}^T\boldsymbol{W}\boldsymbol{\epsilon}.$$

The solution has to satisfy the necessary condition

$$\left(\frac{\partial g}{\partial \boldsymbol{\lambda}}\right)^T = \boldsymbol{0}$$

which gives

$$-\boldsymbol{S}_f^T\boldsymbol{W}(\boldsymbol{h}_e - \boldsymbol{S}_f\boldsymbol{\lambda}) = \boldsymbol{0},$$

and thus

$$\boldsymbol{\lambda} = (\boldsymbol{S}_f^T\boldsymbol{W}\boldsymbol{S}_f)^{-1}\boldsymbol{S}_f^T\boldsymbol{W}\boldsymbol{h}_e.$$

Solution to Problem 9.6

Taking into account that $\boldsymbol{C}\boldsymbol{K} = \boldsymbol{K}\boldsymbol{C} = \boldsymbol{I}_6$, Equation (9.70) can be rewritten in the form

$$\boldsymbol{K}' = \boldsymbol{S}_f(\boldsymbol{S}_f^T\boldsymbol{C}\boldsymbol{S}_f)^{-1}\boldsymbol{S}_f^T\boldsymbol{C}\boldsymbol{K}$$

which, considering the definition (9.55) of weighted pseudo-inverse with weight $\boldsymbol{C}$, can be rewritten as

$$\boldsymbol{K}' = \boldsymbol{S}_f\boldsymbol{S}_f^{\dagger}\boldsymbol{K} = \boldsymbol{P}_f\boldsymbol{K}.$$

Solution to Problem 9.7

Assuming that the screwdriver can move along the slot of the screw, it is worth choosing the constraint frame attached to the screwdriver as in Fig. S9.3.

Natural constraints can be determined first. Motion constraints describe the impossibility to generate arbitrary linear velocities along axes y_c, z_c and

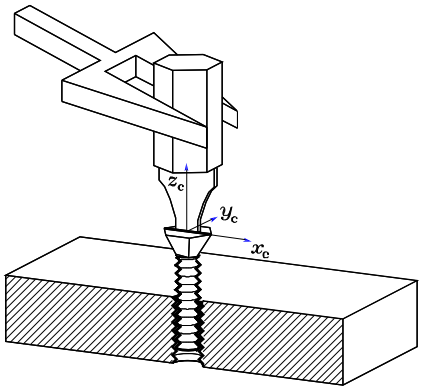

Fig. S9.3. Driving a screw in a hole.

Table S9.1. Natural and artificial constraints for the task of Fig. S9.3.

Natural Constraints	Artificial Constraints
$\dot{p}_y^c$	f_y^c
$\dot{p}_z^c$	f_z^c
ω_x^c	μ_x^c
ω_y^c	μ_y^c
f_x^c	$\dot{p}_x^c$
μ_z^c	ω_z^c

angular velocities about axes x_c, y_c. Force constraints describe the impossibility to exert arbitrary forces along axis x_c and moment about axis z_c.

As a consequence, artificial constraints regard the variables not subject to natural constraints. Hence, with reference to natural velocity constraints along axes y_c, z_c and about x_c, y_c, it is possible to specify artificial constraints for forces along y_c, z_c and moments about x_c, y_c. Also, with reference to natural generalized force constraints along axis y_c and about axis z_c, it is possible to specify artificial constraints for linear velocity along x_c and angular velocity about z_c. The set of constraints is summarized in Table S9.1. Notice that, in the case of a frictionless groove, once ω_z^c is specified, then $\dot{p}_z^c$ is determined according to the pitch of the screw.

Solution to Problem 9.8

The control input (9.77) referred to the constraint frame, in view of the expressions of $\boldsymbol{S}_f^c$, $\boldsymbol{S}_v^c$ and $\boldsymbol{C}'^c$ in Example 9.4, can be computed as

$$\alpha_x^c = \alpha_\nu$$
$$\alpha_y^c = c_{2,2} f_\lambda.$$

Taking into account (9.81), the control input α_y^c can be expressed as

$$\alpha_y^c = -c_{2,2} k_{D\lambda} \dot{\lambda} + k_{P\lambda}(\lambda_d - \lambda),$$

where a constant desired force λ_d was considered. In view of the equalities $\dot{o}_y^c = c_{2,2}\dot{\lambda}$ and $\lambda = f_y^c$, the equation can be rewritten in the form

$$\alpha_y^c = -k_{D\lambda} \dot{o}_y^c + k_{P\lambda}(\lambda_d - f_y^c),$$

showing that the the control action in the force controlled subspace consists of a proportional force control with inner velocity loop.

Solution to Problem 9.9

The computation of $\boldsymbol{S}_f^{c\dagger}$ using the compliance matrix

$$\boldsymbol{C}^c = \begin{bmatrix} c_{1,1} & c_{1,2} \\ c_{1,2} & c_{2,2} \end{bmatrix}$$

as a weighting matrix gives

$$\boldsymbol{S}_f^{c\dagger} = (\boldsymbol{S}_f^{cT} \boldsymbol{C}^c \boldsymbol{S}_f^c)^{-1} \boldsymbol{S}_f^{cT} \boldsymbol{C}^c = \begin{bmatrix} c_{2,2}^{-1} c_{1,2} & 1 \end{bmatrix}.$$

On the other hand, computing $\boldsymbol{S}_f^{\dagger}$ in the base frame gives

$$\boldsymbol{S}_f^{\dagger} = (\boldsymbol{S}_f^T \boldsymbol{C} \boldsymbol{S}_f)^{-1} \boldsymbol{S}_f^T \boldsymbol{C} = \frac{1}{\sqrt{2}} \begin{bmatrix} \dfrac{c_{1,2} - c_{2,2}}{c_{2,2}} & \dfrac{c_{1,2} + c_{2,2}}{c_{2,2}} \end{bmatrix},$$

where $\boldsymbol{C} = \boldsymbol{R}_c \boldsymbol{C}^c \boldsymbol{R}_c^T$. Notice that $\boldsymbol{S}_f^{\dagger} = \boldsymbol{S}_f^{c\dagger} \boldsymbol{R}_c^T$ and the same transformation rule holds for $\boldsymbol{S}_v^{\dagger}$. Also, if $\boldsymbol{f}_e^c = \begin{bmatrix} f_x^c & f_y^c \end{bmatrix}^T$, then

$$\lambda = \boldsymbol{S}_f^{c\dagger} \boldsymbol{f}_e^c = \boldsymbol{S}_f^{\dagger} \boldsymbol{f}_e = \frac{c_{1,2}}{c_{2,2}} f_x^c + f_y^c,$$

independently from the frame to which $\boldsymbol{S}_f^{\dagger}$ and $\boldsymbol{f}_e$ are referred. On the other hand, if the contact force $\boldsymbol{f}_e^c$ belongs to subspace $\mathcal{R}(\boldsymbol{S}_f^c)$, i.e., $\boldsymbol{f}_e^c = \begin{bmatrix} 0 & f_y^c \end{bmatrix}^T$, then it is $\lambda = f_y^c$ independently from the particular weighting matrix.

Analogously, the computation of $\boldsymbol{S}_v^{c\dagger}$ using the stiffness matrix

$$\boldsymbol{K}^c = \begin{bmatrix} k_{1,1} & k_{1,2} \\ k_{1,2} & k_{2,2} \end{bmatrix}$$

as a weighting matrix gives

$$\boldsymbol{S}_v^{c\dagger} = (\boldsymbol{S}_v^{cT} \boldsymbol{K}^c \boldsymbol{S}_v^c)^{-1} \boldsymbol{S}_v^{cT} \boldsymbol{K}^c = \begin{bmatrix} 1 & k_{1,1}^{-1} k_{1,2} \end{bmatrix}$$

in the constraint frame, and

$$\boldsymbol{S}_v^{\dagger} = \frac{1}{\sqrt{2}} \begin{bmatrix} \dfrac{k_{1,1} - k_{1,2}}{k_{1,1}} & \dfrac{k_{1,1} + k_{1,2}}{k_{1,1}} \end{bmatrix}$$

in the base frame.

Solution to Problem 9.10

In view of the results of Example 9.4, the hybrid control law can be designed by choosing the control inputs α_ν and f_λ according to (9.80) and (9.84), respectively, with suitable control gains.

In detail, the control gains in (9.80) can be set to

$$k_{P\nu} = 16 \qquad k_{I\nu} = 100,$$

corresponding to $\omega_{n\nu} = 10\,\text{rad/s}$ and $\zeta_\nu = 0.8$ for the dynamics of the velocity error $\nu_d - \nu$.

The same dynamics can be imposed to the force λ with the choice

$$k_{D\lambda} = 16 \qquad k_{P\lambda} = 100,$$

in the case that the stiffness of the environment is known.

In the case that only an estimate of the stiffness of the environment is available, the quantity $\boldsymbol{L}_f = l_f$ has the value

$$l_f = \frac{\hat{c}_{2,2}}{c_{2,2}}$$

and thus

$$\dot{\hat{\lambda}} = \hat{c}_{2,2}^{-1} \dot{o}_y^c.$$

Assuming, for example, $\hat{c}_{2,2}^{-1} = 4 \cdot 10^3\,\text{N/m}$, then $l_f = 1.25$, corresponding to $\omega_{n\lambda} = 11.18\,\text{rad/s}$ and $\zeta_\lambda = 0.71$ for the dynamics of the force.

The initial tip position is chosen on the plane as $\boldsymbol{o}_e(0) = [\,1 \quad 0\,]^T$. The desired velocity along axis x_c is set as in Problem 9.3, while the desired force along axis y_c is set to $-50\,\text{N}$.

The resulting SIMULINK block diagram is shown in Fig. S9.4. The arm is simulated as a continuous-time system using a variable-step integration method with a minimum step size of 1 ms. All the blocks of the controller are simulated as discrete-time subsystems with the given sampling time of 1 ms.

The files with the solution can be found in Folder `9_10`.

The resulting tip velocity error along x_c and contact force along y_c are shown in Fig. S9.5. It can be verified that the velocity error keeps small during task execution; also, the contact force reaches the desired value at steady state. In Fig. S9.6, the continuous line represents the end-effector path in the base frame, while the dashed line corresponds to the plane at rest. It can be verified that the plane complies during the interaction.

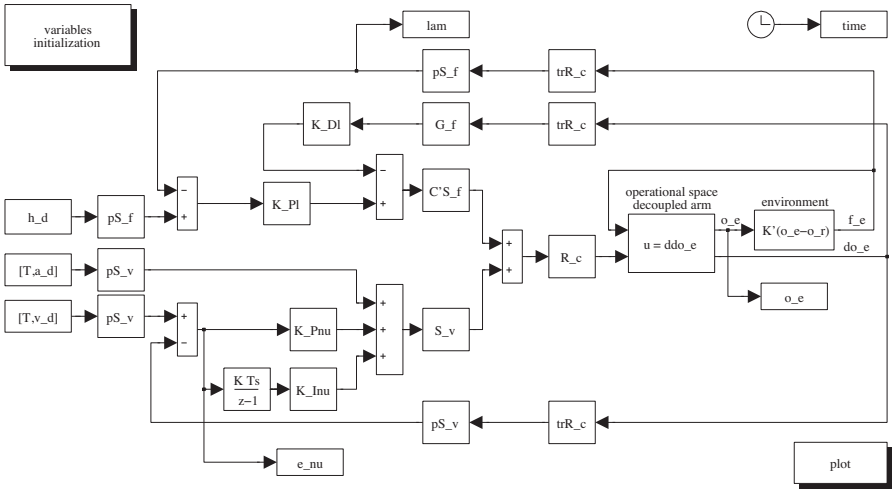

Fig. S9.4. SIMULINK block diagram of hybrid force/motion control.

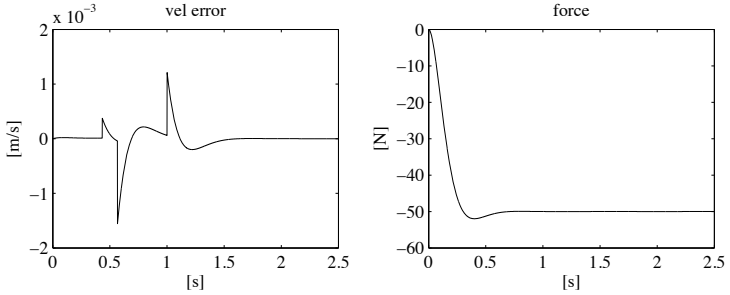

Fig. S9.5. Time history of the tip velocity error and of the contact force with hybrid force/motion control.

Solution to Problem 9.11

In view of equality $\dot{\boldsymbol{q}} = \boldsymbol{J}_\rho(\boldsymbol{r})\dot{\boldsymbol{r}}$ and (9.63) the following equality holds

$$\boldsymbol{v}_e = \boldsymbol{J}(\boldsymbol{q})\dot{\boldsymbol{q}} = \boldsymbol{J}(\boldsymbol{q})\boldsymbol{J}_\rho(\boldsymbol{r})\dot{\boldsymbol{r}} = \boldsymbol{S}_v(\boldsymbol{q})\dot{\boldsymbol{r}}.$$

Hence, pre-multiplying both sides of the above equation by $\boldsymbol{S}_v^\dagger$ and using (9.59) gives

$$\boldsymbol{\nu} = \dot{\boldsymbol{r}}.$$

Also, it is $\dot{\boldsymbol{\nu}} = \ddot{\boldsymbol{r}}$. Therefore, control law (9.95) yields the closed-loop equation

$$\ddot{\boldsymbol{r}} - \ddot{\boldsymbol{r}}_d + \boldsymbol{K}_{Dr}(\dot{\boldsymbol{r}}_d - \dot{\boldsymbol{r}}) + \boldsymbol{K}_{Pr}(\boldsymbol{r}_d - \boldsymbol{r}) = \boldsymbol{0},$$

showing that tracking of a desired position $\boldsymbol{r}_d(t)$ is achieved.

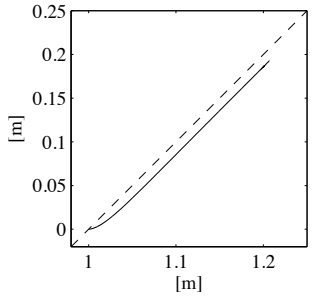

Fig. S9.6. Tip's path in the base frame (continous line) and undeformed contact plane (dashed line).